

# Stochastic resonance-aided energy detection for RF-powered cognitive radio networks

Henry Onyemauche Osuagwu<sup>1</sup>, Mamilus A. Ahaneke<sup>2</sup>, Vincent C. Chijindu<sup>2</sup>, Obinna M. Ezeja<sup>2</sup>

<sup>1</sup>Department of Electrical Engineering, Faculty of Engineering, Nigeria Maritime University, Warri, Nigeria

<sup>2</sup>Department of Electronic and Computer Engineering, Faculty of Engineering, University of Nigeria, Nsukka, Nigeria

## Article Info

### Article history:

Received Oct 10, 2025

Revised Feb 24, 2026

Accepted Mar 29, 2026

### Keywords:

Cognitive radio

Energy detection

Noise uncertainty

Spectrum sensing

Stochastic resonance

## ABSTRACT

Conventional stochastic resonance (SR) techniques often face challenges with higher-frequency signals and parameter optimization for real-time applications, as observed in practical orthogonal frequency-division multiplexing (OFDM) systems that are vulnerable to noise uncertainty (NU). In this study, we present a novel SR-aided energy detection (ED) method that incorporates multi-taper spectrum estimation technique to improve spectrum estimation precision and Gauss-Seidel-like iteration method to accurately adjust the SR parameters for real-time adaptation. This combined strategy enhances weak signal detection, prevents signal distortion, and increases robustness against fluctuating noise conditions. Results from 5,000 Monte Carlo simulations showed that, at 0 dB NU, SR-aided ED attained 90% detection probability at -11 dB, outperforming conventional ED with an SNR gain of 12.5 dB. At 3 dB NU, the conventional ED accuracy degraded by 5.5 dB, resulting in a false alarm probability of 77%, while SR-aided ED demonstrated robustness to NU. At 10 dB NU, ED failed to distinguish the differences between noise and signal power, giving rise to 99% false alarm probability. In contrast, despite a 6 dB degradation, the developed SR-aided ED approach still guarantees a 1% false alarm probability. In clipping-prone systems, conventional ED is vulnerable to signal clipping. Conversely, SR-aided ED remains unaffected.

This is an open access article under the [CC BY-SA](https://creativecommons.org/licenses/by-sa/4.0/) license.



## Corresponding Author:

Henry Onyemauche Osuagwu

Department of Electrical Engineering, Faculty of Engineering, Nigeria Maritime University

Okerenkoko, Warri, Nigeria

Email: henry.osuagwu.pg68120@unn.edu.ng

## 1. INTRODUCTION

The increasing number of wireless communication systems and the rising demand for the limited radio spectrum have resulted in spectrum scarcity. To address spectrum scarcity and the power constraints problems in radio communication systems, an innovative technology known as radio frequency (RF)-powered cognitive radio networks (CRNs) has emerged as highly viable solution. This cutting-edge technology addresses the energy bottleneck of conventional CRNs through allowing the secondary users (SUs) to intelligently monitor and harvest energy from surrounding RF signal [1]. In RF-powered CRNs, spectrum sensing plays an important role in granting secondary (unlicensed) user opportunistic access to unused spectrum without causing interference to primary (licensed) users. However, spectrum sensing faces serious challenges. In low signal-to-noise ratio (SNR) environment, the detection performance degraded notably when implementing conventional energy detection (ED) methods [2]. Noise uncertainty (NU), resulting from environmental fluctuation, hardware imperfection and interference, impacts negatively on spectrum detection accuracy, hence increasing the false alarm probability [3], [4].

Fading and shadowing can conceal weak signals, causing hidden node problems that require complex cooperative sensing algorithms, thereby increasing computational and energy demand [5]. In full-duplex networks, self-interference leaks SU signals into receiving devices [6], concealing the primary user (PU) signals in CRNs. These challenges prevent accurate detection of spectrum holes and expose the PUs to interference. Improving the sensitivity of spectrum detecting devices that can consistently identify spectrum opportunities at very low SNR is crucial for seamless operation of CRNs [7]. Future methodologies for spectrum detection should incorporate diverse strategies to achieve robust performance against NU and signal clipping while guaranteeing false alarm probability that is equal to or less than 10%. This study aims to tackle some of these challenges through stochastic resonance (SR)-aided ED sensing method that employs powerful signal processing techniques that are efficient and adaptive to modern wireless communications technologies. Outlined are the research contributions:

- This study derived mathematical expression of the SNR gain generated through bistable nonlinear systems, that showed how the SR system adapts to varying noise conditions.
- A novel analytical formulation is obtained for the detection probability of SR-aided ED
- It investigates the impact of NU and signal clipping on the detection accuracy of SR-aided ED in low SNR environment.

As follows are the subsequent sections of the paper: section 2 presents the related works. The conventional ED that incorporates NU, signal clipping, SR system, mechanism of multi-taper spectral estimation, SR parameters estimation, the formulation of the SNR gain for SR System, and the analytical model for the detection probability of SR-aided ED are presented in section 3. The results of simulations, the discussion and the developed model comparison with existing published models in literature are provided in section 4. Finally, section 5 presents conclusion reflections.

## 2. RELATED WORKS

In recent times, SR-aided ED technique has mostly focused on improving the spectrum detection accuracy in low SNR environments, which is a major challenge for typical ED method. The investigation in [8] presents cooperative perception algorithm for a few nodes that adopt a single-node sensing scheme in accordance with SR with an improved Quantum Manta-Ray Optimisation. The method improves detection accuracy in low SNR scenarios. The algorithm developed in [9] leverage on customised nonlinear systems to extract weak fault signal concealed in noise, extending beyond conventional SR by adapting potential well structure for effective noise-to-signal transition. Heuristic techniques notably the firefly algorithm (FFA) was developed in [10] to determine the appropriate amount of noise and SR parameters, leading to improve probability of detection (Pd) of the system's weak signal.

An innovative spectrum detection method that employs SR to strengthen primary user's spectrum detection accuracy was presented in [11]. With a constant false alarm probability, the technique detection probability outperforms typical energy detectors in low SNR environments, while maintaining the same computational complexity. Jiang *et al.* [12] suggested an SR-based algorithm for cooperative spectrum sensing in low SNR environments. The technique incorporates technologies that resulted in improved Pd and minimised error rate, specifically for licensed users in cognitive radio. The study in [13] put forward a novel approach leveraging adaptive SR networks, designed to enhance parameter estimation of wireless channel in low SNR environments where typical approaches underperform. The SR network's capability to boost the signal strength through the incorporation of noise is exploited in this approach, thus resulting in improved detection sensitivity.

The challenge of improving spectrum detection in low SNR has been tackled across studies on SR-aided ED. However, several study gaps and unsolved challenges exist in some of the published literature. The existing SR models often consider conceptual additive white Gaussian noise (AWGN) scenarios. Researchers are yet to explore how complex, unpredictable NU, licensed user interference, and signal clipping impacts SR-aided ED accuracy and reliability in fluctuating RF surroundings. The conventional SR systems were designed for straightforward periodic signals; to deal with non-periodic, multi-carrier signals, SR systems require robust approaches.

The SR parameter selection and the accurate estimation of noise power are very important for SR-aided ED algorithm efficiency. In real-world situations, noise intensity fluctuates tremendously in response to the surrounding conditions and interference. Due to the intrinsic NU, it becomes challenging to develop robust SR-aided energy detectors that could perform effectively and appropriately. In this study, we combine multi-taper spectral estimation (MTSE) approach with a Gauss-Seidel-like iteration method in SR-aided ED to address some of these challenges.

### 3. DEVELOPED NETWORK MODEL FOR SR-AIDED ED

The SR-aided ED model shown in Figure 1 is designed for orthogonal frequency-division multiplexing (OFDM) transmissions [14], [15] in AWGN channel, aiming to improve weak signal detection accuracy by precisely injecting noise into the system. A key performance metric for the SR system's efficient operation is the SNR gain, indicating an increased SNR post-SR enhancement.

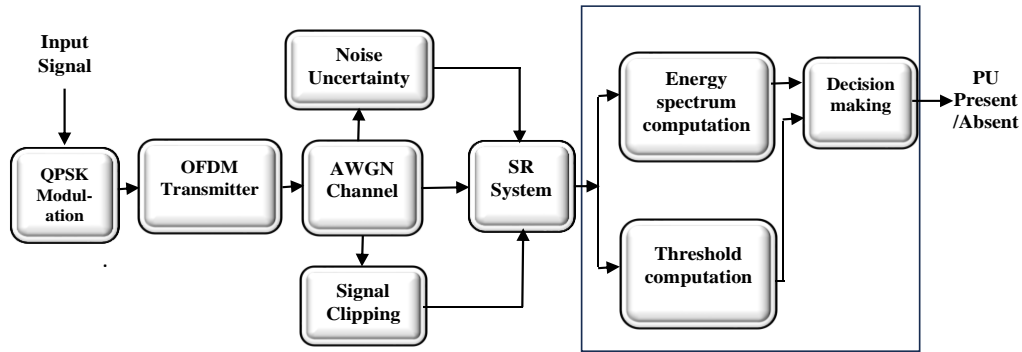


Figure 1. SR-aided ED network model. The model utilizes an input signal, an injected controlled noise source, and a nonlinear bistable system to enhance weak signal detection

#### 3.1. ED that incorporates NU

Accurate noise power estimation is very important for ED systems to perform effectively, while an incorrect estimation results in an increasing probability of false alarm  $P_{fa}$  and undesirable SNR wall [16]. In a situation where there is  $x$  dB of inaccurate measurement of interference and noise power. The probable value of the interference power,  $\sigma_e^2$  can take any number of values between the interval defined by  $\sigma_n^2 10^{-(x/10)}$  and  $\sigma_n^2 10^{(x/10)}$ , expressed as  $\sigma_e^2 \in [10^{-(x/10)} \sigma_n^2, 10^{(x/10)} \sigma_n^2]$  [17]. Where  $\sigma_n^2$  denotes noise variance while  $10^{x/10}$  equate to uncertainty factor,  $\rho$ , of the noise incorporated into the noise model, given a threshold that  $\rho \geq 1$ . It has become common knowledge that the uncertainty factor  $\rho = 1$ , provided there exists no variations in the noise power value [18]. It is possible to define in just one interval the uncertainty that results from the distribution of noise  $\sigma^2 \in [\sigma_n^2/\rho, \rho\sigma_n^2]$ . Thus, the equations defining the  $P_{fa}$  and probability of detection,  $P_d$  for an event that integrates NU are defined as follows [14], [19]:

$$P_{fa} = \max_{\sigma^2 \in [\sigma_n^2/\rho, \rho\sigma_n^2]} Q \left( \frac{\lambda_{ED} - N\sigma_n^2}{\sqrt{2N\sigma_n^4}} \right) = Q \left( \frac{\lambda_{ED} - NNU\rho\sigma_n^2}{\rho\sigma_n^2\sqrt{2NNU}} \right) \quad (1)$$

$$P_d = \min_{\sigma^2 \in [\sigma_n^2/\rho, \rho\sigma_n^2]} Q \left( \frac{\lambda_{ED} - N(\sigma_n^2 + SNR\sigma_n^2)}{\sqrt{2N(\sigma_n^2 + SNR\sigma_n^2)^2}} \right) = Q \left( \frac{\lambda_{ED} - NNU(\sigma_n^2/\rho + SNR\sigma_n^2/\rho)}{\sqrt{2NNU(\sigma_n^2/\rho + SNR\sigma_n^2/\rho)^2}} \right) \quad (2)$$

If  $X$  represents a beta-distributed random variable defined by the shape parameters alpha ( $\alpha$ ) and beta ( $\beta$ ) [20], then the mean is calculated as follows:

$$E(X) = \text{betarnd}(\alpha, \beta) = \frac{\alpha}{\alpha + \beta} \quad (3)$$

The actual noise variance is expected to be distributed within a range determined by a lower bound ( $x_{min} = \sigma_n^2/\rho$ ) and an upper bound ( $x_{max} = \rho\sigma_n^2$ ). We can estimate the noise variance,  $\sigma_n^2$  by incorporating the beta random variable into the uncertainty range  $[x_{min}, x_{max}]$ , which produces one specific variance realisation for  $x$  dB uncertainty thus,

$$\sigma_{n\_NU}^2 = x_{min} + (x_{max} - x_{min}) \times \text{betarnd}(\alpha, \beta) \quad (4)$$

Considering equal parameters ( $\alpha = \beta$ ), the probability distribution is symmetric around the mean of 0.5. Then, (4) is reformulated as:

$$\sigma_{n_{NU}}^2 = \sigma_n^2/\rho + (\rho\sigma_n^2 - \sigma_n^2/\rho) \times 0.5 \quad (5)$$

$$\sigma_{n_{NU}}^2 = \frac{\sigma_n^2(1+\rho^2)}{2\rho} \quad (6)$$

$\sigma_{n_{NU}}^2$  represent noise variance that incorporates NU. We use (6) to simulate a fluctuating noise variance by applying beta distribution. It precisely quantifies uncertainty by adapting the beta-distributed random variable to the interval  $[x_{min}, x_{max}]$ . This approach allows for achievable Monte Carlo simulations by mimicking the unpredictability nature of real-world noise.

### 3.2. Signal clipping

Clipping induces signal distortion and degradation. To restrict a signal when it crosses a specific threshold, the threshold must be lower than the signal's highest point for clipping to hold true. Figure 2 shows clipping in a three-dimensional (3-D) visualisation. The basic concept of the clipping signal approach involves establishing the clipping threshold at the signal's peak amplitude prior to any processing.

- a. Firstly, we analyse the entire modulated signal to find its peak absolute value of the amplitude.

$$Amplitude_{peak} = \max(|s(t)|)$$

- b. We defined the clipping threshold,  $T_c$ , equal to the peak amplitude, thus

$$T_c = Amplitude_{peak}$$

- c. Finally, we clip the signal by applying hard clipping to each sample of the signal,  $s(t)$ , according to the following function, which makes the output signal  $y(t)$  [21]:

$$y(t) = T_c \text{ if } s(t) > T_c$$

$$y(t) = -T_c \text{ if } s(t) < -T_c$$

$$y(t) = s(t) \text{ if } |s(t)| \leq T_c$$

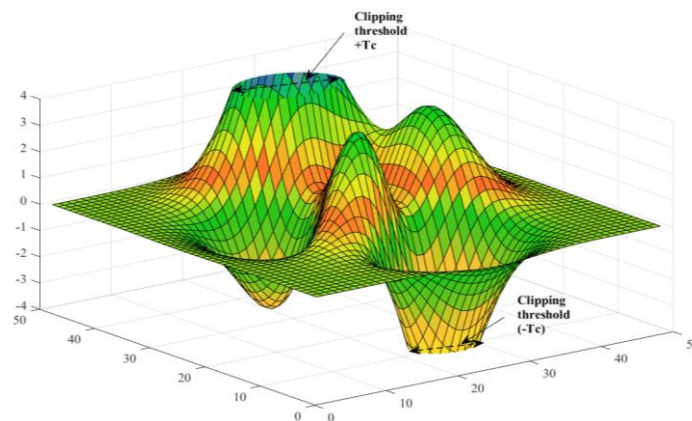


Figure 2. Three-dimensional plot of clipped signal

### 3.3. SR system

A stochastic differential equation (SDE), such as the Langevin equation for a bistable potential is used to represent the SR system, which is the main component of the method. A nonlinear system described in [22] with evenly distributed double well potentials is represented by  $U(x, t)$ .

$$U(x, t) = -\frac{a}{2}x(t)^2 + \frac{b}{4}x(t)^4 \quad (7)$$

The parameters  $a$  and  $b$  of the SR system are responsible for determining the dimensions and depth of the potential well [23], where  $a, b > 0$ . When an input periodic weak signal at time  $t$ ,  $s(t) = A\cos(2\pi f_0 t)$ , and

Gaussian noise  $n(t)$  are applied to this bistable system, the conventional overdamped bistable SR has the form thus [22], [24]:

$$\frac{dx(t)}{dt} = -\frac{\partial U(x,t)}{\partial x} + s(t) + n(t) \quad (8)$$

The amplitude of the weak periodic signal is denoted as  $A$ , and  $f_0$  is the driving frequency. The two stable positions of bistable system are  $\pm x = \pm\sqrt{a/b} = \pm c$ , and when the potential height centered at the origin,  $x_0 = 0$ , the barrier height  $U_0 = \Delta U = a^2/4b$ . The condition  $r_K = 2f_0$  according to the two-state theory SR, refers to “stochastic matching,” where the mean waiting time ( $1/r_K$ ) for noise-driven transitions matches half the period ( $1/f_0$ ) of the ambient signal [25]. This synchronisation optimises the system’s response to a weak periodic or aperiodic signal in the presence of noise. Where  $r_K$  is the Kramers rate and is defined as:

$$r_K = \frac{a}{\sqrt{2\pi}} \exp\left(-\frac{\Delta U}{D}\right) \quad (9)$$

$D$  is the Gaussian white noise intensity. A typical simplified equation derived from two-state theory relating SNR to  $r_K$  is:

$$SNR = \frac{\pi A^2 r_K}{4D^2} \quad (10)$$

In (10) states that in a bistable SR system, SNR is directly proportional to  $r_K$  of state transition, it predicts a maximum SNR output at a specific noise intensity. In this study, the fourth-order Runge-Kutta (RK4) technique [26] is employed to model the bistable SR system. The SDE under investigation is:

$$\frac{dx(t)}{dt} = \frac{dy}{dt} = f(y, t) + s(t) + n(t) = ay - by^3 + s(t) + n(t) \quad (11)$$

Where  $s(t)$ ,  $y(t)$  are the input and output signal at the SR system respectively.  $a, b$  are potential barrier SR parameter, and  $n(t) = \sqrt{D}\xi(t)$  is the noise input,  $\xi(t)$  represents Gaussian white noise with zero mean and unit variance. To estimate the signal output at the SR system quantitatively, we apply RK4 approach with a step size  $h$ . Finding the four successive slopes ( $K_1, K_2, K_3, K_4$ ) results in the recursive discrete iteration of the present value  $y_n$  to the subsequent value  $y_{n+1}$ .

$$\begin{cases} K_1 = h[ay_n - by_n^3 + s_n + n_n] \\ K_2 = h\left[a\left(y_n + \frac{k_1}{2}\right) - b\left(y_n + \frac{k_1}{2}\right)^3 + s_n + n_n\right] \\ K_3 = h\left[a\left(y_n + \frac{k_2}{2}\right) - b\left(y_n + \frac{k_2}{2}\right)^3 + s_{n+1} + n_n\right] \\ K_4 = h[a(y_n + K_3) - b(y_n + K_3)^3 + s_{n+1} + n_n] \\ y_{n+1} = y_n + \frac{1}{6}(K_1 + 2K_2 + 2K_3 + K_4) \end{cases} \quad (12)$$

### 3.4. Mechanism of the multi-taper spectral estimation

Prior to SR processing, a MTSE technique was utilised to improve spectrum estimation precision, aimed at reducing the high variance and spectral leakage problems inherent in single-taper methods. The MTSE technique estimates the power spectral density (PSD) of a signal [27] by averaging many modified periodograms calculated, each with a distinct taper [28], [29]. The optimised spectrum is subsequently used for the adaptive selection of SR parameters using the Gauss-Seidel-like iteration method. The MTSE processes of the input signal used in this study are as follows:

- For  $i = 1, \dots, 4$ , received signal  $y[n]$  through the noise channel of the total length  $L_{total}$  is divided into adjacent segments  $y_i[n]$ :

$$y_i = y\left[n + \frac{(i-1)L_{total}}{4}\right], \quad 0 \leq n < \frac{L_{total}}{4} \quad (13)$$

- The PSD of each segment  $y_i[n]$  is estimated by applying the multi-taper method. The estimate  $E_i(f)$  for segment  $i$  with a time-bandwidth product  $NW_i$  can be described as the mean of  $K_i \approx [2NW_i - 1]$  distinct “eigen taper” estimates:

$$E_i(f) = \frac{1}{K_i} \sum_{k=0}^{K_i-1} \left[ \sum_{n=0}^{L/4-1} w_{n,k}(NW_i) * y_i[n] \exp^{-2\pi f n} \right]^2 \quad (14)$$

Where  $w_{n,k}(NW_i)$  denotes the Slepian tapers [27], [30], [31]. The decision to choose  $K = 2NW - 1$  tapers guarantee only sequences with high energy density across the band of frequencies  $(-W, W)$ . The variable  $NW$  represents the estimated frequency density,  $N$  denotes the number of samples,  $W$  denotes the needed amount of bandwidth. To reduce spectral leakage, adaptive multi-taper estimation with specific weights  $w_{n,k}(f)$  according to the eigenvalue  $\lambda_K$  across the band of frequencies  $(-W, W)$  of each Slepian taper or discrete prolate spheroidal sequence (DPSS) is defined thus:

$$w_{n,k}(f) = \frac{\lambda_K}{[\lambda_K \tilde{S}(f) + (1 - \lambda_K) \sigma_n^2]^2} \quad (15)$$

where  $\tilde{S}(f)$  is the tapered periodograms.

c. We sum the estimated PSD to obtain averaged spectrum  $M_{Average}(f)$ .

$$M_{Average}(f) = \sum_i^4 E_i(f) = E_1 + E_2 + E_3 + E_4 \quad (16)$$

d. The destination variable  $M_{input}$  is determined from the portion of the summed spectrum and stored for simulation or analysis.  $M_{input} = \{M_{Average}(f) | f \in N_{trained\ sample}\}$  indicates that the model's input  $M_{input}$  is generated by applying an averaged spectrum function  $M_{Average}$  on each distinct sample in the training set  $N_{trained\ sample}$ . Where  $N_{trained\ sample}$  is a specific number of time-domain training samples, corresponding to the system's fast fourier transformation (FFT) size, that uses controlled randomness to push an SR system into a state of optimal performance and for determining ideal values of  $a$ ,  $b$  and  $D$ . The FFT sizes are generally a power of 2 (e.g., 256, 512, 1024, 2048).

The MTSE process above integrates spatial smoothing through segmentation and spectral smoothing by carrying out variable multi-tapering. The multi-taper method optimises SNR estimation by offering high quality PSD, adaptable weighting for optimal result in fluctuating noise environments.

### 3.5. Estimation of SR parameters

The estimation of optimal SR parameters is often expressed as an *argmax* operation in relation to SNR gain. We perform the optimization process as follows:

$$\theta_{opt} = \underset{\theta}{\operatorname{argmax}} f(\theta) = \underset{\theta}{\operatorname{argmax}} SNR\ output \quad (17)$$

where  $\theta$  is the set of SR parameters  $a$ ,  $b$ , and  $D$  to be estimated,  $f$  is the objective function for the output SNR or SNR gain. The SR parameters are updated successively using a Gauss-Seidel-like iteration method [32], wherein the value of  $k$ -th parameter reusing the most recently estimated values of the remaining parameters. The iterative estimation is predicated on the empirical detection probability,  $P_d$ . Using MATLAB to calculate the detection threshold  $\lambda$ , for the system parameters, we consider the number of training samples  $N_{trained\ sample}$ , and the false alarm probability,  $Pfa$ , by applying a Chi-square distribution,

$$\lambda = \operatorname{chi2inv}(1 - Pfa, N_{trained\ sample}) \quad (18)$$

For a set of probable values  $z \in H$  (where  $H = \{0.01, \dots, 1\}$ ), we computed the numerical  $P_d$  by taking the average of  $N$  test result.

$$P_d(z) = \frac{1}{N} \sum_{i=1}^N |\sum |SR_{out}|^2 \geq \lambda) \quad (19)$$

where  $|\cdot|$  denotes the indicator function,  $SR_{out} = y_{SR}$  is the signal output of the Runge-Kutta 4th-order solver. The first raw estimated value of  $a_{raw}$  is determined across the evaluation space  $H$  based on combined total detection probabilities:

$$a_{raw} = H([\sum_{z \in H} P_d(z)]) \quad (20)$$

Finally, if the variation in  $P_d$  ( $\Delta P_d(z) > 0.2$ ), a small correction is added to  $a_{raw}$ .

$$a_{k+1} = a_{raw} + 0.05$$

The value of the parameter  $a_{k+1}$  is first updated using the initial values  $b_k$  and  $D_k$ . The parameter  $b_{k+1}$  subsequently gets estimated, using the most recent estimated  $a_{k+1}$  and  $D_k$ . The parameter  $D_{k+1}$  is estimated lastly, using the newly calculated values  $a_{k+1}$  and  $b_{k+1}$ .

### 3.6. Formulation of the SNR gain for SR system

The average SNR at the input of SR system is,

$$SNR_{input} = \frac{A_m^2}{2\sigma_n^2} \quad (21)$$

The optimum SNR gain can be attained through the dynamic adjustments of the added variance of the noise power  $\sigma_{n_0}^2$  with the variable  $U_0$ . The SNR output at SR system is calculated thus [33]:

$$SNR_{output} = \frac{4\sqrt{2}A_m^2U_0}{(\sigma_n^2 + \sigma_{n_0(opt)}^2)^2} e^{-2U_0/(\sigma_n^2 + \sigma_{n_0(opt)}^2)} \quad (22)$$

The optimum value of  $\sigma_{n_0(opt)}^2$  can potentially be derived by setting the derivative of SNR output with respect to  $\sigma_{n_0}^2$  to zero,  $(\partial SNR_{output}/\partial \sigma_{n_0}^2) = 0$ . We achieved this optimisation by an analytical method that determines the ideal settings that improve SNR gain. The product rule in calculus is applied for (22) to get the differential equation between two functions that are multiplied together. Let,

$$u = \frac{4\sqrt{2}A_m^2U_0}{(\sigma_n^2 + \sigma_{n_0(opt)}^2)^2}, v = \exp^{-2U_0/(\sigma_n^2 + \sigma_{n_0(opt)}^2)} \text{ and } SNR_{output} = uv$$

$$\frac{\partial SNR_{output}}{\partial \sigma_{n_0}^2} = \frac{4\sqrt{2}A_m^2U_0}{(\sigma_n^2 + \sigma_{n_0(opt)}^2)^2} \times \frac{2U_0}{(\sigma_n^2 + \sigma_{n_0(opt)}^2)^2} \exp^{-2U_0/(\sigma_n^2 + \sigma_{n_0(opt)}^2)} + \exp^{-2U_0/(\sigma_n^2 + \sigma_{n_0(opt)}^2)} \times$$

$$\frac{8\sqrt{2}A_m^2U_0(\sigma_n^2 + \sigma_{n_0(opt)}^2)}{(\sigma_n^2 + \sigma_{n_0(opt)}^2)^4} = 0 \quad (23)$$

$$\frac{8\sqrt{2}A_m^2U_0^2}{(\sigma_n^2 + \sigma_{n_0(opt)}^2)^4} \exp^{-2U_0/(\sigma_n^2 + \sigma_{n_0(opt)}^2)} = \frac{8\sqrt{2}A_m^2U_0(\sigma_n^2 + \sigma_{n_0(opt)}^2)}{(\sigma_n^2 + \sigma_{n_0(opt)}^2)^4} \exp^{-2U_0/(\sigma_n^2 + \sigma_{n_0(opt)}^2)} \quad (24a)$$

$$U_0 = \sigma_n^2 + \sigma_{n_0(opt)}^2 \quad (24b)$$

From (24b), the optimum theoretical value of  $\sigma_{n_0(opt)}^2$  is determined, giving us the result.

$$\sigma_{n_0(opt)}^2 = U_0 - \sigma_n^2 \quad (25)$$

It is possible to evaluate the SNR gain through incorporating the following (21), (22), and (24b).

$$SNR_{gain} = \frac{SNR_{output}}{SNR_{input}} = \frac{8\sqrt{2}\sigma_n^2}{\exp^2 U_0} \quad (26)$$

The effective manipulation of the SR variable  $U_0$  can guarantee a higher SNR output than the SNR input ( $SNR_{output}/SNR_{input} > 1$ ), if

$$U_0 > \frac{8\sqrt{2}\sigma_n^2}{\exp^2} \quad (27)$$

where the potential barrier height,  $U_0 = a^2/4b$ .

### 3.7. A novel analytical model for the detection probability of SR-aided ED

In an analytical approach of SR-aided ED, a nonlinear system is used to improve the detection probability of weak signals. This is accomplished by transitioning the energy of noise into the energy of valuable signals. The mathematical equations of SR-aided ED offer important understanding of the internal processes and factors necessary for optimising the detection accuracy of a poor signal. In (2) represents the probability of detecting the conventional ED for an event that incorporates NU. The SNR in (2) is the average SNR at the input ( $SNR_{input}$ ) of SR system. From (26), the SNR at the output of the SR system is calculated as follows.

$$SNR_{output} = \frac{8\sqrt{2}\sigma_n^2}{\exp^2 U_0} \times SNR_{input} \quad (28)$$

By incorporating (28) into (2), a novel analytical expression for SR-aided ED is developed.

$$P_{d\_SR} = Q \left( \frac{\lambda_{ED} - N_{NU} \left( \sigma_n^2 / \rho + \frac{8\sqrt{2}\sigma_n^4 SNR_{input}}{exp^2 U_0 \rho} \right)}{\sqrt{2N_{NU} \left( \sigma_n^2 / \rho + \frac{8\sqrt{2}\sigma_n^4 SNR_{input}}{exp^2 U_0 \rho} \right)^2}} \right) \quad (29)$$

where  $P_{d\_SR}$  is the detection probability of SR-aided ED. Using a straightforward energy detector method, the test statistic  $T_{S\_SR}$  for SR-aided ED can easily be computed.

$$T_{S\_SR} = \sum_{n=1}^N |y(t)_{SR}|^2 \quad (30)$$

where  $y(t)_{SR}$  represents the signal output from the SR system. Test statistics, or calculated energy, are compared to the predefined ED threshold  $\lambda_{ED}$ .

- If  $T_{S\_SR} > \lambda_{ED}$ , signal is present.
- If  $T_{S\_SR} \leq \lambda_{ED}$ , signal is absent.

For a specific  $P_{fa}$  value, the ED sensing threshold  $\lambda_{ED}$  is computed as follows:

$$\lambda_{ED} = (Q^{-1}(P_{fa})\sqrt{2N} + N)\sigma_n^2 \quad (31)$$

### 3.8. Flow chart for simulating the developed SR-aided ED process

Figure 3 illustrates the flow chart of SR-aided energy detector that incorporates MTSE approach with Gauss-Seidel-like iteration method. The diagram provides a systematic overview of the entire process, starting from the initial signal acquisition to the final decision-making stage. Furthermore, the flowchart highlights the integration of SR parameters optimization as a critical step in enhancing the detection of weak signals.

### 3.9. Simulation's parameters

In this study, simulations are done with MATLAB version 2024b simulator and 5,000 Monte Carlo simulations were run to achieve the desired outcome. For simulation parameters, see Table 1. These parameters are carefully selected to reflect the standard specifications of an OFDM-based communication system under various SNR conditions. The use of a high number of iterations ensures the statistical reliability of the results and minimizes the potential for detection errors.

Table 1. Simulation parameters

Parameters	Type/Value
Bandwidth/Subcarrier spacing	10 MHz/15 KH
Carrier frequency offset (CFO)	0.3
PU signal transmission type	OFDM
Radio frame length	10 ms
Number of transmitting antennas	1
Number of receiving antennas	1
FFT size	1024
OFDM Symbols	14
Number of training samples	512
OFDM type (constellation)	QPSK
Number of cyclic prefixes	7
Noise channel model	AWGN
Probability of false alarm	0.1
Number of Monte Carlo simulations	5,000
The SNR value at the point of detection of the SU	-15 and -10 dB
Step size $h$	0.1
SR parameters $a, b$ and $D$	Dynamically estimated
Target $P_d$ and $P_{fa}$	90% and 0.1

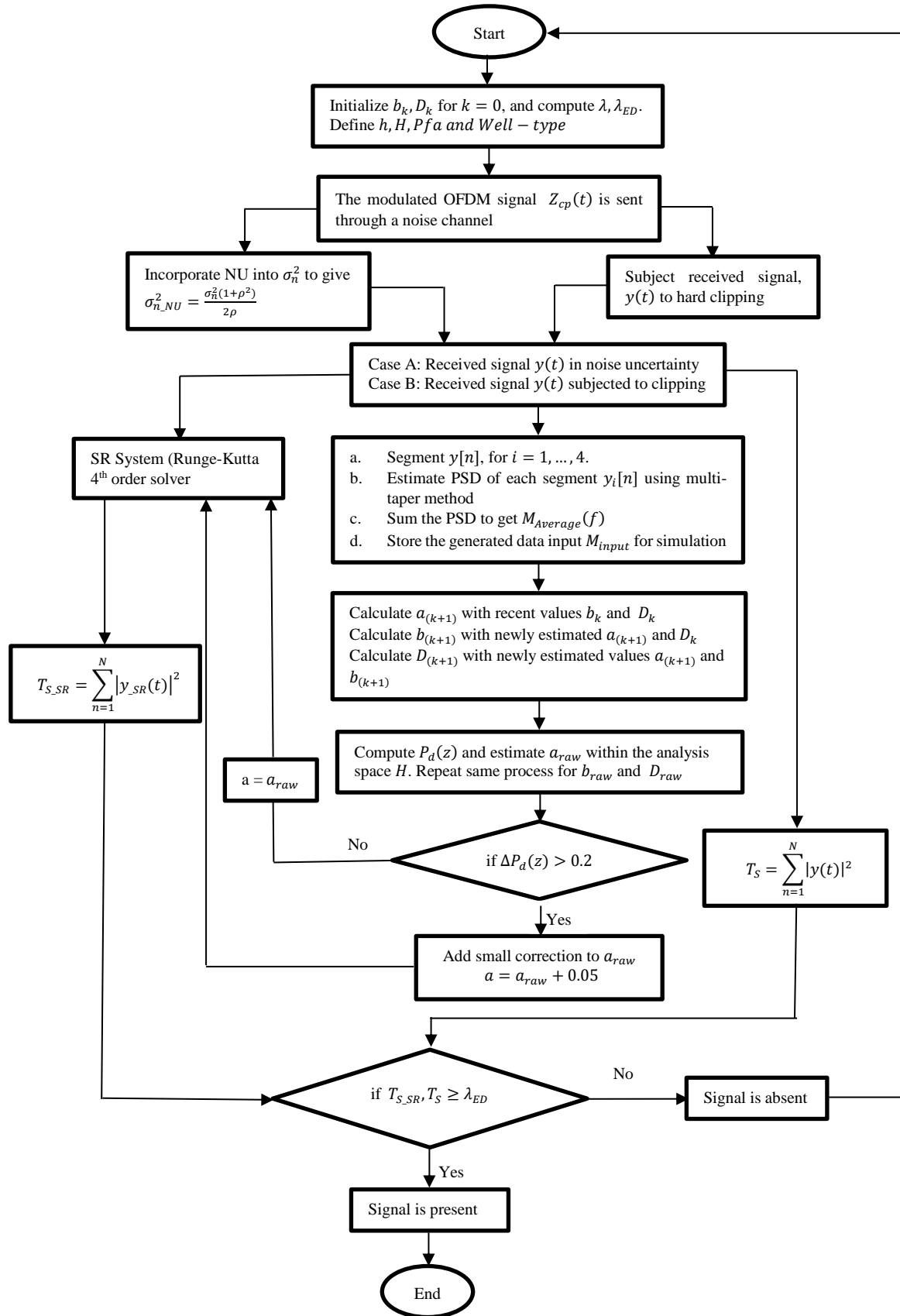


Figure 3. The flow chart of the developed SR-aided ED. The process starts with signal processing, followed by signal analysis and SR parameters optimization, energy calculation and decision-making process for weak signal detection

## 4. RESULTS AND DISCUSSION

### 4.1. Plot of output SNR against noise intensity

The output SNR against noise intensity  $D$  typically exhibits a bell-like shape curve reaching its peak at optimal noise intensity. As shown in Figure 4, the variation in SR parameter 'b' is often connected to potential barrier slope. A higher 'b' promotes optimization of SR system ability to detect weak signal, leading to improved maximum attainable SNR and performance enhancement in low noise environments. A decreasing 'b' requires more background noise to induce transition, leading to decreased peak SNR output and faster performance degradation.

### 4.2. Receiver operating characteristics (ROC) curve

The variation in the probabilities of detection in relation to the false alarm probability at SNR = -15 dB and -10 dB is illustrated in Figure 5. The performance comparison of the developed SR-aided ED and the conventional ED in relation to the ROC curve was demonstrated. Higher SNR indicates increased probability of detection. The  $P_d$  improves with an increase in false alarm probability at a given SNR value. Observe that as the SNR decreases, the overall performance approaches to a potential diagonal where  $P_d = P_{fa}$ . Under the same false alarm probability conditions, the developed SR-aided ED outperforms the conventional ED.

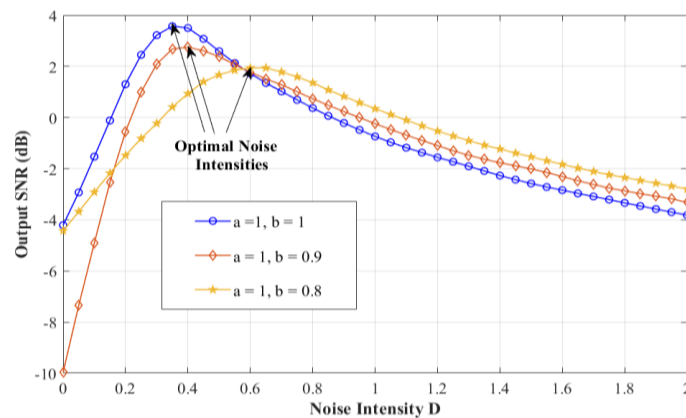


Figure 4. Variation of the output SNR against noise intensity ( $D$ ) at varied SR parameter ( $b = 0.8, 0.9, \text{ and } 1$ ) with fixed value  $a = 1$

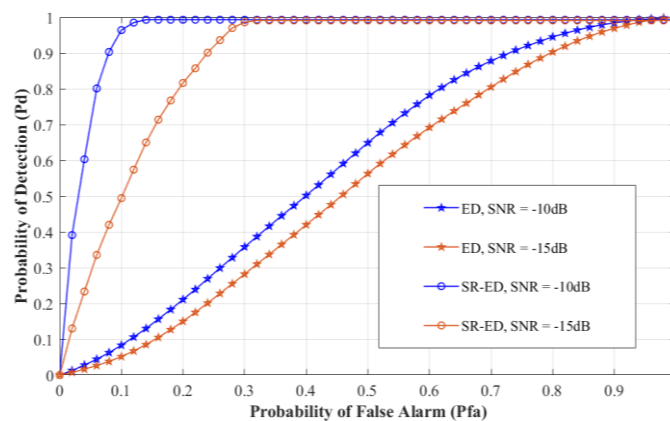


Figure 5. Plot of ROC curves in AWGN. The graph depicts the  $P_d$  versus false alarm probability ( $P_{fa}$ ) for SNR = -15 dB and -10 dB

### 4.3. Plot of simulation and theoretical results of SR-aided ED

Validating the developed SR-aided ED model demands comparing theoretical data with simulated outcomes, to support comprehension of the system's functionality under varying conditions. The detection probability of the theoretical SR-aided ED is a numerically calculated value generated from statistical algorithms and system hypotheses, optimally designed for performance under ideal conditions. In contrast, the

simulated results of the detection probability are obtained using Monte Carlo simulations that account for unpredictable conditions, with more investigation resulting in better accurate performance. The comparison of theoretical and simulation data confirms the accuracy of the developed model and guides its implementation in a specific set of conditions. The discrepancies between simulation and theoretical results, as depicted in Figure 6, represent not a deficiency but an inherent aspect that helps with model validation, which reveals real-world phenomena such as signal distortion and CFO that are absent in the theoretical algorithm.

#### 4.4. Performance of SR-ED and ED in NU

NU in receiving equipment can range from 1 to 2 dB, impacting ED spectrum sensing methods. Incorrect noise power calculations can affect ED functionality. As shown in Figure 7, at 0 dB NU, SR-aided ED achieved 90% detection probability at -11 dB with a 12.5 dB SNR gain. At 3 dB NU the energy-based detection degrades by 5.5 dB, leading to high false alarm rates of 77%. SR-aided ED, on the other hand, shows robustness at 3 dB NU. At 10 dB NU, the conventional ED method is ineffective in identifying the difference between noise and signal power, triggering 99% false alarm probability. Though the developed SR-aided ED degraded by 6 dB, it still guarantees 1% false alarm probability.

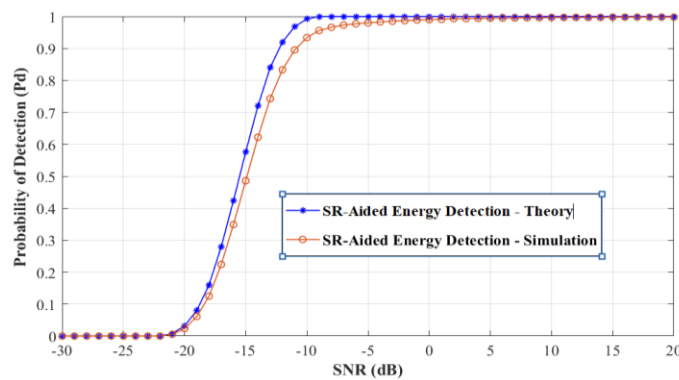


Figure 6. Plot of Pd versus SNR (dB) for SR-aided ED. It illustrates comparison between the simulation results and theoretical predictions at  $Pfa = 0.1$

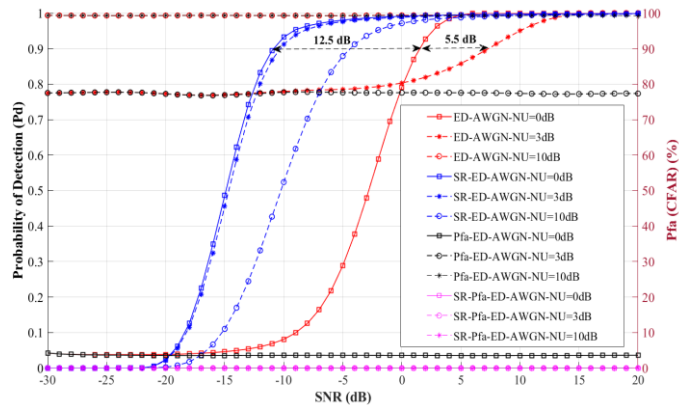


Figure 7. Plot of Pd versus SNR (dB) under variable NU. The graphs depict performance at NU values of 0 dB (Ideal), 3 dB and 10 dB. Simulations were run with a constant  $Pfa = 0.1$

#### 4.5. Performance of SR-aided ED and the conventional ED when the modulated signal is clipped

Figure 8 shows the impact of subjecting modulated signal to clipping at varying levels of 0%, 30%, 50%, 70%, and 100%, for both conventional ED and the developed SR-aided ED. While the percentage of the clipping threshold of modulated signal increases, the conventional ED method Pd degrades until the detection probability dropped to zero at 100% clipping threshold. In contrast, the developed SR-aided ED shows robustness to clipping at varied threshold levels, which confirms its capability to distinguish between signal and noise power in communication systems.

#### 4.6. Developed model comparison with existing published model in the literatures

Table 2 presents a comparison between the developed model and the experimental results reported in [3], [34] for the single-input-single-output (SISO)-OFDM and  $2 \times 2$  multiple-input-multiple-output (MIMO)-OFDM systems, with a predetermined probability of false alarm,  $P_{fa} = 0.1$ . Table 2 illustrates how MIMO networks significantly improve detection probability in ED relative to single input single output (SISO) networks by using transmission diversity and spatial data. This improvement is apparent owing to MIMO's reliability and its use of multiple antennas that boost efficiency and robustness. MIMO systems, at a target probability of 90%, achieve better detection accuracy in low SNR conditions at -3 dB, outperforming SISO networks. However, MIMO systems increased power consumption owing to additional antennas, complex RF and signal processing circuits, and extra processing components. In performance comparisons of the developed SISO SR-aided ED model against an energy-based detector for MIMO-OFDM systems in [34]. The developed model achieves a better SNR gain of 12.5 dB with low power consumption due to single antenna implementation, outperforming the MIMO-OFDM model in [34] that presents a 7.5 dB SNR gain.

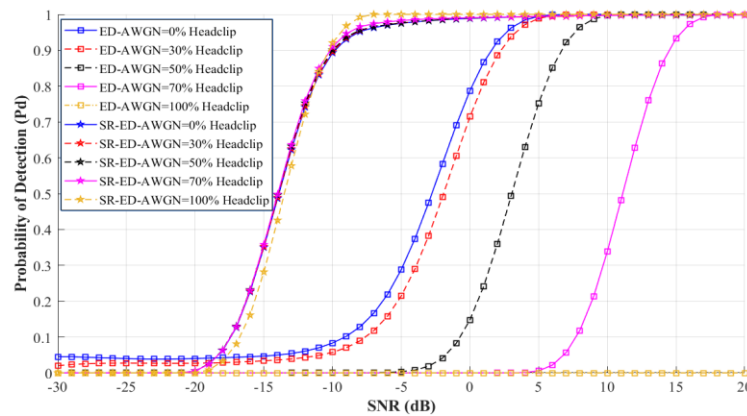


Figure 8. Plot of performance comparison of SR-aided ED and the conventional ED methods under hard clipping distortion. The graphs show the impact of varied clipping levels (between 0 and 100%) on Pd versus SNR (dB), evaluated at 0 dB NU

Table 2. Developed model comparison with existing models in literature

Number of antennas and reference	Modulation type	Number of sample/OFDM symbols	False alarm probability, $P_{fa}$ at NU = 0	SNR at target $P_d = 90\%$
Conventional ED SISO-OFDM	QPSK	1024	0.05	1.5dB
SISO-OFDM [34]	QPSK	1024	0.01	4.5dB
MIMO-OFDM [34]	QPSK	1024	0.01	-3dB
Developed SR-aided ED SISO-OFDM	QPSK	1024	0.01	-11dB

## 5. CONCLUSION

This study presents a novel, highly precise spectrum detection methodology for SR-aided energy detectors that combine MTSE technique with an iterative Gauss-Seidel-like method to improve detection performance and reduce NU impacts. The derived Pd for the SR-aided ED method was validated by comparing the theoretical and simulated results, hence confirming the accuracy of the analytical model formulation. Simulation findings show that the model is adaptive to NU, attaining high detection accuracy in extremely low SNR environments while guaranteeing a false alarm probability of 1%. The developed model proves robustness to signal clipping, establishing its capability to distinguish between signal and noise power in communication systems. This study also demonstrate how properly controlled noise can raise weak signals above detection threshold, making them detectable. Such findings are especially important for 5G networks, where signals are vulnerable to interference caused by geographic constraints. Implementing SR as an initial processing stage may improve SNR prior to detection, resulting in better signal reception and overall system efficiency.

While the combined MTSE and Gauss-Seidel-like iteration techniques for SR-aided ED shows the potential to improve weak signal detection in CRNs. Future research will focus on its implementation in hardware platforms, such as a Software Defined Radio (SDR), to evaluate the technique in practical applications. The study will be extended to include more complex fading channels for realistic simulations.

Further research will be conducted to investigate the incorporation of this methodology into a corporative spectrum sensing framework that involves multiple SUs.

### FUNDING INFORMATION

This research received a complete funding from the Federal Government of Nigeria through the TETFUND grant for PhD studies, sponsored by Nigeria Maritime University, Okerenkoko, Warri, Nigeria.

### AUTHOR CONTRIBUTIONS STATEMENT

This journal uses the Contributor Roles Taxonomy (CRediT) to recognize individual author contributions, reduce authorship disputes, and facilitate collaboration.

Name of Author	C	M	So	Va	Fo	I	R	D	O	E	Vi	Su	P	Fu
Henry Onyemauche Osuagwu	✓	✓	✓	✓	✓	✓	✓	✓	✓	✓	✓		✓	✓
Mamilus A. Ahaneku		✓				✓		✓		✓	✓	✓		
Vincent C. Chijindu		✓				✓				✓	✓	✓		
Obinna M. Ezeja						✓				✓	✓		✓	

C : Conceptualization

M : Methodology

So : Software

Va : Validation

Fo : Formal analysis

I : Investigation

R : Resources

D : Data Curation

O : Writing - Original Draft

E : Writing - Review & Editing

Vi : Visualization

Su : Supervision

P : Project administration

Fu : Funding acquisition

### CONFLICT OF INTEREST STATEMENT

No conflict of interest.

### DATA AVAILABILITY

The data that support the findings of this study are available on request from the corresponding author, [HOO].




### REFERENCES

- [1] S. Böhm and H. König, "Radio-in-the-loop simulation and emulation modeling for energy-efficient and cognitive internet of things in smart cities: a cross-layer optimization case study," *Computer Communications*, vol. 218, pp. 157–165, Mar. 2024, doi: 10.1016/j.comcom.2024.02.006.
- [2] A. S. S. Musuvathi, J. F. Archbald, T. Velmurugan, D. Sumathi, S. Renuga Devi, and K. S. Preetha, "Efficient improvement of energy detection technique in cognitive radio networks using K-nearest neighbour (KNN) algorithm," *EURASIP Journal on Wireless Communications and Networking*, vol. 2024, no. 1, p. 10, Feb. 2024, doi: 10.1186/s13638-024-02338-8.
- [3] J. Lorincz, I. Ramljak, and D. Begušić, "Analysis of the impact of detection threshold adjustments and noise uncertainty on energy detection performance in MIMO-OFDM cognitive radio systems," *Sensors*, vol. 22, no. 2, p. 631, Jan. 2022, doi: 10.3390/s22020631.
- [4] Md. S. Miah, M. Schukat, E. Barrett, M. M. Cespedes, and A. G. Armada, "Enhanced spectrum sensing for AI-enabled cognitive radio IoT with noise uncertainty," *ITU J-FET*, vol. 6, no. 1, pp. 76–91, Mar. 2025, doi: 10.52953/weqd6699.
- [5] T. Balachander, K. Ramana, R. M. Mohana, G. Srivastava, and T. R. Gadekallu, "Cooperative spectrum sensing deployment for cognitive radio networks for internet of things 5G wireless communication," *Tsinghua Science and Technology*, vol. 29, no. 3, pp. 698–720, Jun. 2024, doi: 10.26599/TST.2023.9010065.
- [6] X. Zhang, Y. Liu, P. Yang, and C. Gao, "Full-duplex DF relay sensing-communication integration via self-interference echo serial decoupling," *Journal of Information and Intelligence*, Nov. 2025, doi: 10.1016/j.jiixd.2025.10.005.
- [7] S. Islam, A. Kumar Budati, M. Kamrul Hasan, S. Mahfoudh, and S. Bilal Hussian Shah, "Performance analysis of three spectrum sensing detection techniques with ambient backscatter communication in cognitive radio networks," *Computer Modeling in Engineering & Sciences*, vol. 137, no. 1, pp. 813–825, 2023, doi: 10.32604/cmescs.2023.027595.
- [8] J. Chen, Y. Huang, T. Wang, L. Zhang, and Y. Li, "Performance evaluation of cooperative spectrum sensing algorithm based on quantum manta ray algorithm," *IEEE Access*, vol. 13, pp. 185169–185180, 2025, doi: 10.1109/ACCESS.2024.3416464.
- [9] J. Liu, J. Guo, B. Hu, Q. Zhai, C. Tang, and W. Zhang, "Controlled symmetry with woods-Saxon stochastic resonance enabled weak fault detection," *Sensors*, vol. 23, no. 11, p. 5062, May 2023, doi: 10.3390/s23115062.
- [10] H. T. Reda, A. Mahmood, A. Diro, N. Chilamkurti, and S. Kallam, "Firefly-inspired stochastic resonance for spectrum sensing in CR-based IoT communications," *Neural Computing and Applications*, vol. 32, no. 20, pp. 16011–16023, Oct. 2020, doi: 10.1007/s00521-019-04584-0.
- [11] D. He, Y. Lin, C. He, and L. Jiang, "A novel spectrum-sensing technique in cognitive radio based on stochastic resonance," *IEEE*




- Transactions on Vehicular Technology*, vol. 59, no. 4, pp. 1680–1688, May 2010, doi: 10.1109/TVT.2010.2042311.
- [12] B. Jiang, Y. Cao, J. Bao, C. Liu, and X. Tang, “Novel piecewise normalized bistable stochastic resonance strengthened cooperative spectrum sensing,” *IEEE Transactions on Cognitive Communications and Networking*, vol. 9, no. 5, pp. 1167–1182, Oct. 2023, doi: 10.1109/tccn.2023.3287236.
- [13] D. He, P. Wang, and W. Yu, “Stochastic-resonance-networks-enhanced wireless channel parameter estimation approach,” *IEEE Internet of Things Journal*, vol. 11, no. 8, pp. 14313–14327, Apr. 2024, doi: 10.1109/JIOT.2023.3340893.
- [14] J. Lorincz, I. Ramljak, and D. Begušić, “A review of the noise uncertainty impact on energy detection with different OFDM system designs,” *Computer Communications*, vol. 148, pp. 185–207, Dec. 2019, doi: 10.1016/j.comcom.2019.09.013.
- [15] K. Shrivastav, “Phase noise in OFDM,” in *Multiplexing - Recent Advances and Novel Applications*, IntechOpen, 2022, doi: 10.5772/intechopen.105551.
- [16] Yonghong Zeng and Ying-chang Liang, “Eigenvalue-based spectrum sensing algorithms for cognitive radio,” *IEEE Transactions on Communications*, vol. 57, no. 6, pp. 1784–1793, Jun. 2009, doi: 10.1109/TCOMM.2009.06.070402.
- [17] Jun Ma, G. Y. Li, and Bing Hwang Juang, “Signal processing in cognitive radio,” *Proceedings of the IEEE*, vol. 97, no. 5, pp. 805–823, May 2009, doi: 10.1109/JPROC.2009.2015707.
- [18] G. Mahendru, A. Shukla, and P. Banerjee, “A novel mathematical model for energy detection based spectrum sensing in cognitive radio networks,” *Wireless Personal Communications*, vol. 110, no. 3, pp. 1237–1249, Feb. 2020, doi: 10.1007/s11277-019-06783-3.
- [19] J. Lorincz, I. Ramljak, and D. Begušić, “A survey on the energy detection of OFDM signals with dynamic threshold adaptation: open issues and future challenges,” *Sensors*, vol. 21, no. 9, p. 3080, Apr. 2021, doi: 10.3390/s21093080.
- [20] K. Hornik, “Two monotonicity results for beta distribution functions,” *Entropy*, vol. 26, no. 11, p. 938, Oct. 2024, doi: 10.3390/e26110938.
- [21] C. Gaultier, S. Kitić, R. Gribonval, and N. Bertin, “Sparsity-based audio declipping methods: selected overview, new algorithms, and large-scale evaluation,” *IEEE/ACM Transactions on Audio, Speech, and Language Processing*, vol. 29, pp. 1174–1187, 2021, doi: 10.1109/taslp.2021.3059264.
- [22] J. Li, Y. Zhang, and P. Xie, “A new adaptive cascaded stochastic resonance method for impact features extraction in gear fault diagnosis,” *Measurement*, vol. 91, pp. 499–508, Sep. 2016, doi: 10.1016/j.measurement.2016.05.086.
- [23] S. Sun, X. Qi, Z. Yuan, X. Tang, and Z. Li, “Power system signal-detection method based on the accelerated unsaturated stochastic resonance principle,” *Applied Sciences*, vol. 14, no. 10, p. 4284, May 2024, doi: 10.3390/app14104284.
- [24] C. Ji, Q. Zhao, Y. Yu, and W. Dai, “Detection of weak signals under low SNR stochastic resonance system,” *IEEE Access*, vol. 11, pp. 101881–101889, 2023, doi: 10.1109/ACCESS.2023.3284319.
- [25] M. Xu, C. Zheng, K. Sun, L. Xu, Z. Qiao, and Z. Lai, “Stochastic resonance with parameter estimation for enhancing unknown compound fault detection of bearings,” *Sensors*, vol. 23, no. 8, p. 3860, Apr. 2023, doi: 10.3390/s23083860.
- [26] A. G. Shaikh, U. Keerio, W. Shaikh, and A. H. Sheikh, “Numerical higher-order Runge-Kutta methods in transient and damping analysis,” *International Journal of ADVANCED AND APPLIED SCIENCES*, vol. 9, no. 10, pp. 174–179, Oct. 2022, doi: 10.21833/ijaas.2022.10.020.
- [27] Inc. The MathWorks, “pmtm - Multitaper power spectral density estimate,” May 24, 2025. [Online]. Available: <https://uk.mathworks.com/help/signal/ref/pmtm.html>
- [28] G. A. Prieto, R. L. Parker, D. J. Thomson, F. L. Vernon, and R. L. Graham, “Reducing the bias of multitaper spectrum estimates,” *Geophysical Journal International*, vol. 171, no. 3, pp. 1269–1281, Oct. 2007, doi: 10.1111/j.1365-246X.2007.03592.x.
- [29] D. J. Thomson, “Spectrum estimation and harmonic analysis,” *Proceedings of the IEEE*, vol. 70, no. 9, pp. 1055–1096, 1982, doi: 10.1109/JPROC.1982.12433.
- [30] J. L. Romero and M. Speckbacher, “Spectral-norm risk rates for multi-taper estimation of Gaussian processes,” *Journal of Nonparametric Statistics*, vol. 34, no. 2, pp. 448–464, Apr. 2022, doi: 10.1080/10485252.2022.2071888.
- [31] A. A. Patil, G. M. Eadie, J. S. 佳士 Speagle 沆, and D. J. Thomson, “Improving power spectrum estimation using multitapering: efficient asteroseismic analyses for understanding stars, the milky way, and beyond,” *The Astronomical Journal*, vol. 168, no. 5, p. 193, Nov. 2024, doi: 10.3847/1538-3881/ad7029.
- [32] H. Zhou, Z. Xu, X. Liu, and X. Zhang, “A robust and generalized gauss-seidel solver for physically-correct simultaneous collisions,” *Proceedings of the ACM on Computer Graphics and Interactive Techniques*, vol. 8, no. 1, pp. 1–17, May 2025, doi: 10.1145/3728291.
- [33] S. Zhang, J. Wang, M. Zhong, and S. Li, “Adaptive stochastic resonance aided energy detection with modified periodogram,” in *2013 International Conference on Communications, Circuits and Systems (ICCCAS)*, IEEE, Nov. 2013, pp. 72–76, doi: 10.1109/ICCCAS.2013.6765189.
- [34] J. Lorincz, I. Ramljak, and D. Begušić, “Performance analyses of energy detection based on square-law combining in MIMO-OFDM cognitive radio networks,” *Sensors*, vol. 21, no. 22, p. 7678, Nov. 2021, doi: 10.3390/s21227678.

## BIOGRAPHIES OF AUTHORS






**Henry Onyemauche Osuagwu**    obtained a B.Eng. in Electronic Engineering and M.Eng. in Communication Engineering from the University of Nigeria, Nsukka, Enugu State, Nigeria. He is completing his Ph.D. in the Department of Electronic and Computer Engineering at the University of Nigeria, Nsukka. He is also a member of teaching staff in the Department of Electrical Engineering at Nigeria Maritime University, Okerenkoko, Warri, Nigeria. He is a member of Nigeria Society of Engineers and a registered member of COREN (Council for the Regulation of Engineering in Nigeria). His research interests include wireless communication networks, wireless sensor networks, renewable energy, machine learning and the internet of things. A significant number of his research contributions have been published in journals that are reputable. He can be contacted at email: henry.osuagwu.pg68120@unn.edu.ng.






**Mamilus A. Ahaneku**    received his B. Eng (Electrical and Electronic Engineering) and M.Sc. (Communications Engineering) from Federal University of Technology Owerri, Imo State, Nigeria. He obtained his Ph.D. in Communications Engineering from University of Nigeria, Nsukka in 2015. He is a Professor of Communications Engineering, University of Nigeria Nsukka, Enugu State, Nigeria. He has successfully supervised many Ph.D. and master's Students. His research interests include wireless communication, renewable energy, microwaves system, radio frequency design and internet of things (IoT) and image processing. He is a member of Nigerian Society of Engineers and Nigerian Institute of Electrical and Electronic Engineers. He has published over 50 papers in reputable, high impact journals. He can be contacted at email: [mamilus.ahaneku@unn.edu.ng](mailto:mamilus.ahaneku@unn.edu.ng).



**Vincent C. Chijindu**    obtained his B.Eng. (Electrical and Electronic Engineering) and M.Eng. (Computer Science and Engineering) from Anambra State University of Technology Enugu and Enugu State University of Science and Technology, respectively. He obtained his Ph.D. in Computer Engineering from Nnamdi Azikiwe University, Awka, Anambra State, Nigeria in 2016. He is an Associate Professor of Computer Engineering, University of Nigeria Nsukka, Enugu State, Nigeria. He has successfully supervised and graduated 3 Ph.D. and 7 master's Students, while currently supervising a handful of students at both the master's and Ph.D. levels. His research interests include digital image processing, machine learning and artificial intelligence, renewable energy systems and materials, wireless sensor networks and systems. He received the Certificate of Merit award as the Best Graduating Student in the Department of Electrical and Electronic Engineering, Anambra State University of Technology in 1988. He is a member of Nigerian Society of Engineers, IEEE Nigeria Section, and Nigeria Computer Society (NCS). He has over 45 journal publications and one patented work to his credit. He can be contacted at email: [vincent.chijindu@unn.edu.ng](mailto:vincent.chijindu@unn.edu.ng).



**Obinna M. Ezeja**    received his Ph.D. in Communications Engineering from the Department of Electronic and Computer Engineering, Faculty of Engineering, University of Nigeria, Nsukka. Prior to this, he obtained his M. Eng. (Communications Engineering), and B. Eng. from the same department and institution. Furthermore, he is a senior lecturer in the department and has also successfully supervised graduate and undergraduate research and project works. He is currently the coordinator of graduate studies in the department. In addition, he has published many peer-reviewed journal articles and conference papers. His current research interests include machine learning based wireless sensor networks optimization studies. He is also a registered member of COREN (Council for the Regulation of Engineering in Nigeria). He can be contacted at email: [obinna.ezeja@unn.edu.ng](mailto:obinna.ezeja@unn.edu.ng).